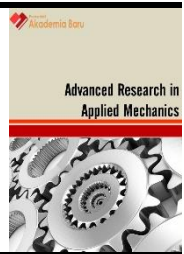




## Journal of Advanced Research in Applied Mechanics

Journal homepage:  
<http://www.akademiarbaru.com/submit/index.php/aram/index>  
ISSN: 2289-7895



# Modelling of Nanomaterial Growth with Flame Enhancement

Muhammad Daffa Naufal<sup>1</sup>, Mohd Fairus Mohd Yasin<sup>1,\*</sup>, Nor Azwadi Che Sidik<sup>2</sup>

<sup>1</sup> High Speed Reacting Flow Laboratory (HIREF), School of Mechanical Engineering, Faculty of Engineering, Universiti Teknologi Malaysia, 81310 Johor Bahru, Johor, Malaysia

<sup>2</sup> Department of Mechanical Precision Engineering, Malaysia-Japan International Institute of Technology, University Technology Malaysia, Jalan Sultan Yahya Petra, 54100 Kuala Lumpur, Malaysia

### ABSTRACT

Flame synthesis offers great potential for a more economical production of Carbon Nanotubes dCNTs because of its rapid process. However, majority of CNT flame synthesis research is geared towards experimental study and modelling studies are limited. Experimental studies come with limitations such as being too costly and time consuming. Utilizing CFD can provide efficiency and introduce data in early stages of research. There are a number of modelling studies that model CNT synthesis in non-premixed flames, but modelling studies that model CNT growth in premixed flames are still sparse. The flame parameters are also quite vast that influence CNT growth in flames, and experimental setups are time and cost consuming. There are also limitations of experimental instrumentations in terms of temporal and spatial resolution which hinders detailed analysis of CNT growth. Synthesis limits are also sensitive to equivalence ratio. The present study aims on modelling the combustion reaction that take place in CNT synthesis in premixed flames with a multi-scale modelling approach. This is done by developing a baseline model of flame synthesis of CNTs in premixed flames using CFD. The CFD results serve as an input for an established growth rate model that predicts CNT length. The range of equivalence ratios ( $\phi$ ) used in the present study are from 1.4 to 2.2, with increments of 0.2. The lowest average CNT length was  $15\mu\text{m}$  at  $\phi = 1.4$ , and the highest being  $26.6\mu\text{m}$  at  $\phi = 2.2$ . This falls in line with the theory that growth rate increases with equivalence ratio due to increased carbon supply. It was also found that the growth temperature range tends to narrow down as equivalence ratio increases. This is because as the equivalence ratio increases, the concentration of optimum carbon precursor tends to be more concentrated a specific region. This study investigates CNT growth in premixed flames by analyzing the temperature and species mass fraction due to limitations in validating the flame model which hinders spatial analysis.

#### Keywords:

Flame Synthesis; Premixed Flame; CFD;  
CNT Length; Equivalence Ratio

Received: 23 February 2022   Revised: 16 March 2022   Accepted: 18 March 2022   Published: 20 March 2022

## 1. Introduction

### 1.1 Background of CNTs

Carbon Nanotubes (CNTs) are nanostructures that are made up of carbon and have a tubular shape. CNTs exhibit various magnificent mechanical and electrical properties due to the carbon atoms arranged in a hexagonal manner, which results in CNTs exhibiting high tensile strength and Young's Modulus [1]. The average tensile strength and Young's modulus for SWCNTs are 13-52 GPa and 320-1470 Gpa respectively [2], whereas for MWCNTs, average tensile strength and Young's modulus values lie in between 11-63 GPa and 270-950 GPa. In terms of thermal properties, CNTs exhibit a thermal conductivity of 3000 W/mK [3] and a melting point between 2600K and 4800K [4].

\* Corresponding author.

E-mail address: [mohdfairus@mail.fkm.utm.my](mailto:mohdfairus@mail.fkm.utm.my)

With their excellent thermal, mechanical and electrical properties, it offers a number of potential uses including the fabrication of composite materials, such as field-effect transistors, , battery electrodes, sensors and probes, catalyzers for fuel cells, targeted drug delivery, tissue engineering, and high-capacity storage media [1], [5].

When it comes to production of CNTs, there are currently four common methods for it. These methods include arc discharge, laser ablation, flame synthesis and chemical vapour deposition (CVD) [6]. CNTs are usually produced by chemical vapour deposition (CVD), however it is an expensive method because it requires heating a furnace. Flame synthesis offers great potential for more cost-efficient production of CNTs as it is faster and requires less energy [7]. However, the temperature gradient within the flame causes difficulties in controlling flame synthesis parameters, making mass production a challenge.

Flame models are beneficial and could also be used to link flame parameters to an established growth rate model. A computational fluid dynamics (CFD) simulation is an essential tool for modeling fluids and observing their behavior. CNT morphology, growth density and internal structures are usually defined in terms of flame gas chemical compositions and usually varied by their fuel-to-air equivalence ratio ( $\phi$ ) [8]. A study by Woo et. al implied that limits are sensitive to fuel-equivalence ratio variation, forming soot rather than CNTs [9].

## 2. Methodology

### 2.1 Overall Methodology

CFD models with varied equivalence ratios are validated by thermodynamic analysis to ensure that the flame model is relevant. This is done by calculating adiabatic flame temperatures ( $T_{ad}$ ) at various equivalence ratios and comparing it with the temperature from CFD results. The equivalence ratios used range from 1.4 to 2.2, with increments of 0.2. The CO<sub>2</sub> mass fractions of the model are validated by comparing between predicted CO<sub>2</sub> by mass fraction analysis and by CFD. The numerical conditions and geometry of the simulation are based on an in-house synthesis experiment using premixed flame. Since the flame is assumed to be symmetrical, only half of the geometry would be employed with a fixed growth time of 3 minutes. The case of equivalence ratio of 1.8 is treated as the baseline case in the present study. The equivalence ratios of each case are varied by varying the respective oxygen concentrations. CFD computations are carried out in ANSYS Fluent 19.2 using a pressure-based solver where the species model employs the partially premixed combustion model which is based on the flamelet solver with the  $k$ - $\epsilon$  turbulence model. Meshing was done for the simulation domain which resulted in approximately 25,000 cells as seen on Figure 1.



**Fig. 1.** The dimensions of computational domain of the baseline premixed flame. Dimensions are in mm and not to scale.

An established growth rate model developed by Zainal [10] would be used in order to predict the CNT length grown over the specified growth time, solved using MATLAB.

$$\frac{dn_1}{dx} = F_{c1} - \frac{n_1}{\tau_{res}} - R_{d,out} - \sigma_x D_s n_1 n_x - (i + 1) \sigma_i D_s n_{f1} n_i - \phi_{c1} \left( \frac{n_{p1} + n_{p2}}{\alpha_m n_m A_{np}} \right) \quad (1)$$

## 2.2 Numerical Conditions

Table 1 and Table 2 denote the respective boundary conditions for the baseline case ( $\phi=1.8$ ).

**Table 1**

Boundary condition for baseline case.

Boundary	Mass Flow Rate (kg/s)	Hydraulic Diameter (m)	Gauge Pressure (Pa)	Mean Mixture Fraction	Progress Variable
Fuel-Air Inlet	$2.98 \times 10^{-5}$	0.017	-	1	1
Shield Inlet	$1.16023 \times 10^{-4}$	0.028	-	0	0
Outlet	-	0.046	0	0	1

**Table 2**

Mass Fraction of Fuel and Oxidizer.

Species	Fuel	Oxidizer
	Mass Fraction	Mass Fraction
CH <sub>4</sub>	0.149	0
O <sub>2</sub>	0.331	0
N <sub>2</sub>	0.519	1

## 3. Results

### 3.1 Boundary Conditions for varied equivalence ratio

Table 1 denotes the boundary conditions for the parametric study on the effects of premixed flame synthesis of CNTs with varied equivalence ratio.

**Table 3**

Numerical conditions for study of effects varied equivalence ratio on CNT growth

Equivalence Ratio	O <sub>2</sub> mass fraction	CH <sub>4</sub> mass fraction	N <sub>2</sub> mass fraction	Flowrate at Inlet (kg/s)	Case Name
1.4	0.390	0.136	0.474	$3.26 \times 10^{-5}$	Case 1.4
1.6	0.358	0.143	0.498	$3.10 \times 10^{-5}$	Case 1.6
1.8	0.331	0.149	0.519	$2.98 \times 10^{-5}$	Case 1.8
2.0	0.308	0.155	0.537	$2.88 \times 10^{-5}$	Case 2.0
2.2	0.289	0.159	0.552	$2.80 \times 10^{-5}$	Case 2.2

### 3.2 Validation based on thermodynamic analysis

Based on Figure 2(a), there is a good agreement between the CFD temperatures and calculated  $T_{ad}$ . Based on Figure 2(b), it can be seen that the flame front gives off a conical shape, but however in the real in-house experiment the flame shape is actually flat instead of conical. This is due to the inability to model, the sintered metal used in the actual experiment, which generates the flat flame shape. The flamelet solver is also unable to model the aerodynamics, & reaction rate that produces the flat shape.

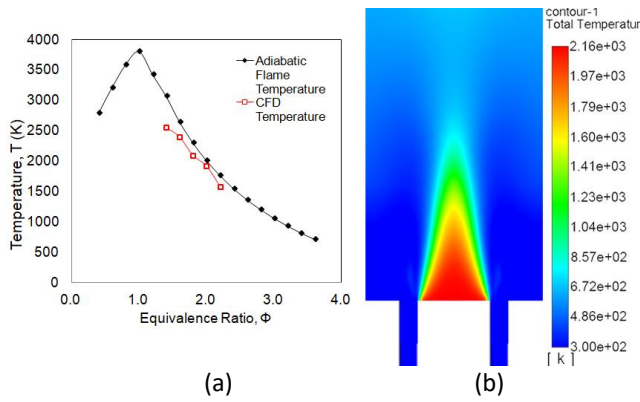


**Fig. 2.** (a) Comparison of calculated  $T_{ad}$  and (b) CFD temperature at  $\phi = 1.4$  to  $\phi = 2.2$  and contour of temperature distribution at  $\phi = 1.8$ .

### 3.3 $CO_2$ Mass Fraction Validation

The analytical  $CO_2$  mass fractions were calculated for each case by mass fraction analysis. Based on Figure 3, it can be seen that the  $CO_2$  mass fraction values from CFD follows the trend where the analytical values decrease with increasing equivalence ratio hence bringing it to a good agreement between the mass fractions, with the difference caused by considering species dissociation in CFD.

### 3.4 Overall Map of CNT length and global flame characteristics

Figure 4 depicts a map of CNT length that is placed side-by-side with the temperature contour of the baseline case to better visualize the CNT growth inside the flame. The left and right half of the flame domain represents contours of temperature and CNT length respectively. The red, orange and yellow contours denote areas of significant CNT growth in the CNT length contour. Conversely, it is assumed that the blue regions denote the areas of no CNT growth. The growth region tends to increase in radial size as the axial distance increases, which can be indicated by observing the increasing temperature distribution becoming wider. However as it reaches the flame tip, the growth region decreases due to the decreasing temperature distribution.

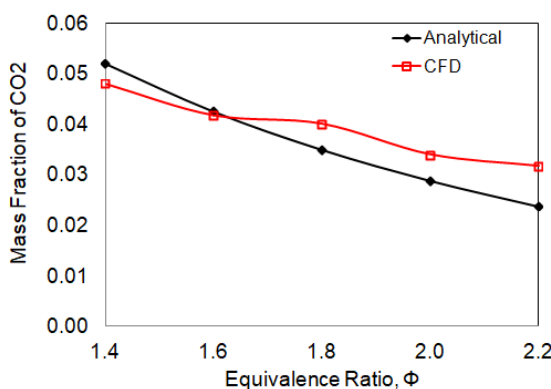


**Fig.3.** Comparison of predicted  $CO_2$  by theoretical calculation and by CFD at  $\phi = 1.4$  to  $\phi = 2.2$

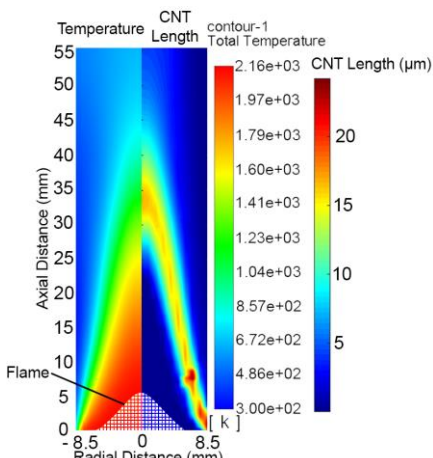


**Fig.4.** Mapping of CNT length at  $\phi = 1.8$  and comparison with temperature distribution.

### 3.4 Effects of varied equivalence ratio on CNT growth

Based on Figure 5(a) and (b), it can be seen that as equivalence ratio increases, there is a steady increase in the average of the highest CNT lengths, with the lowest CNT length at  $\phi = 1.4$  ( $15\mu\text{m}$ ) and the highest CNT length at  $\phi = 2.2$  ( $26.6\mu\text{m}$ ). For the baseline case  $\phi = 1.8$ , the predicted average CNT length was  $23.5 \mu\text{m}$ .

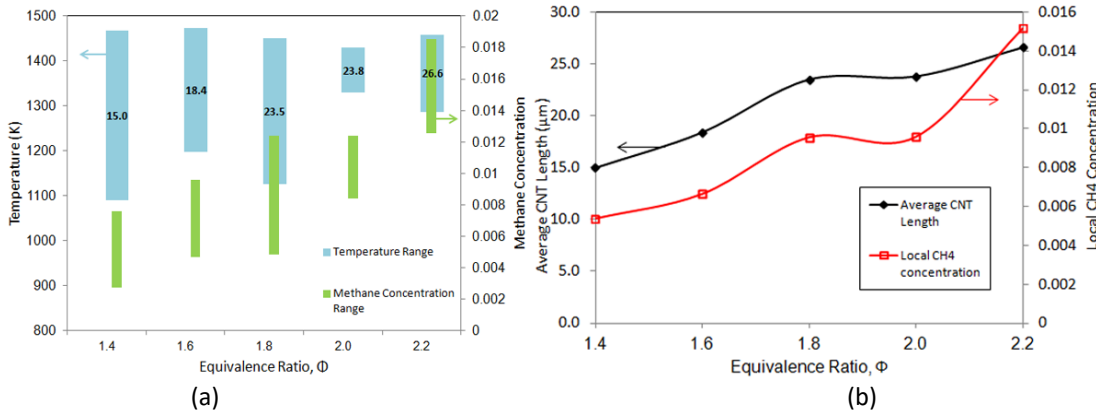


**Fig. 5.** (a) Temperature and methane concentration ranges and respective CNT lengths at  $\phi = 1.4$  to  $\phi = 2.2$ . The numbers inside the blue boxes denote respective CNT lengths for each case in  $\mu\text{m}$  and (b) average CNT lengths and local methane concentrations at  $\phi = 1.4$  to  $\phi = 2.2$ .

CNTs are expected to grow in flames at temperatures from 1000 to around 1400 K [11]–[13], because methane tends to decompose favourably at temperatures above 870 K [14]. The growth rate model computed majority of the significant CNT lengths at temperature ranges where the maximum is around 1450 K. In Figure 5(a), it can be seen that the growth rate model predicted the widest growth temperature range but the lowest CNT length for  $\phi = 1.4$ , and the narrowest growth temperature range at  $\phi = 2.0$ .

Another observation that can be seen in Figure 5(a) is that at  $\phi = 1.4$ , CNTs are able to be grown at temperatures as low as 1100 K, and that they are able to be grown at higher temperatures at  $\phi = 2.2$ . The lower boundary for the temperature range tends to be high when the equivalence ratio is above 2.0. The baseline case has both a wide temperature and methane concentration range, providing flexibility in CNT growth temperature. Based on Figure 5(b) it can be seen that the maximum CNT length from each case increases with equivalence ratio and the local average corresponding methane concentration. The observation falls in line with the theory that higher equivalence ratios tend to be favourable because of the high carbon supply [15].

#### 4. Conclusions

The present study models the flame synthesis of CNTs in premixed flames. Since the flame synthesis process is divided into two scales, the flame scale and particle scale, the CFD model is developed to establish the baseline case of premixed flame model and a growth rate model is utilized in order to predict CNT growth in premixed flames. The effects of varied equivalence ratio of CNT growth in premixed flames are also studied. For the baseline case  $\phi = 1.8$ , the predicted average CNT length was  $23.5 \mu\text{m}$ . The lowest average CNT length was found to be at case  $\phi = 1.4$ , with a length of  $15\mu\text{m}$ , and the highest was found to be at case  $\phi = 2.2$ , with a length of  $26.6\mu\text{m}$ . This falls in line with the theory that growth rate increases with equivalence ratio due to higher carbon supply. As the equivalence ratio increases, the concentration of optimum carbon precursor tends to be more concentrated a specific region.

## Acknowledgement

This research was supported by the Ministry of Education (MOE) through the Fundamental Research Grant Scheme [FRGS/1/2020/TK0/UTM/02/54] with cost center number R.J130000.7851.5F377 and [FRGS/1/2019/TK05/UTM/02/8] with cost center number R.J130000.7851.5F182. The research is also funded by Universiti Teknologi Malaysia (UTM) through the UTM Fundamental Research [UTMFR:PY/2019/01657] grant with cost center number Q.J130 0 0 0.2551.21H10. Authors also would like to thank Universiti Teknologi Malaysia for the funding from Takasago R.K130000.7343.4B732.

## References

- [1] V. N. Popov, "Carbon nanotubes: Properties and application," *Mater. Sci. Eng. R Reports*, vol. 43, no. 3, pp. 61–102, 2004, doi: 10.1016/j.mser.2003.10.001.
- [2] M. F. Yu, B. S. Files, S. Arepalli, and R. S. Ruoff, "Tensile loading of ropes of single wall carbon nanotubes and their mechanical properties," *Phys. Rev. Lett.*, vol. 84, no. 24, pp. 5552–5555, 2000, doi: 10.1103/PhysRevLett.84.5552.
- [3] P. Kim, L. Shi, A. Majumdar, and P. L. McEuen, "Thermal transport measurements of individual multiwalled nanotubes," *Phys. Rev. Lett.*, vol. 87, no. 21, pp. 215502-1–215502–4, 2001, doi: 10.1103/PhysRevLett.87.215502.
- [4] K. Zhang, G. Malcolm Stocks, and J. Zhong, "Melting and premelting of carbon nanotubes," *Nanotechnology*, vol. 18, no. 28, 2007, doi: 10.1088/0957-4484/18/28/285703.
- [5] N. Maheshwari, N. Maheshwari, V. Dhote, and D. K. Mishra, *Carbon Nanotubes and Drug Delivery*. Elsevier Inc., 2020.
- [6] J. P. Gore and A. Sane, *Flame Synthesis of Carbon Nanotubes*, vol. 772. 2011.
- [7] H. Wong Shi Kam, N. ; O'Connell, M.; Wisdom, J. A.; Dai, "Carbon nanotubes as multifunctional biological transporters and near-infrared agents for selective cancer cell destruction," *Social Psychiatr.*, vol. 34, no. 290, pp. 40–44, 2014, doi: 10.1016/j.spsy.2013.10.009.
- [8] R. L. Vander Wal, L. J. Hall, and G. M. Berger, "The chemistry of premixed flame synthesis of carbon nanotubes using supported catalysts," *Proc. Combust. Inst.*, vol. 29, no. 1, pp. 1079–1085, 2002, doi: 10.1016/S1540-7489(02)80136-5.
- [9] S. K. Woo, Y. T. Hong, and O. C. Kwon, "Flame-synthesis limits and self-catalytic behavior of carbon nanotubes using a double-faced wall stagnation flow burner," *Combust. Flame*, vol. 156, no. 10, pp. 1983–1992, 2009, doi: 10.1016/j.combustflame.2009.07.003.
- [10] M. T. Zainal, "Modelling the flame synthesis of carbon nanotube (CNT) in inverse diffusion flame," Universiti Teknologi Malaysia, 2017.
- [11] N. B. I. N. Hamzah, "Analysis of Carbon Nanotube synthesis in methane diffusion flame declaration of thesis / postgraduate project report," *PhD Thesis*, pp. 47–133, 2020.
- [12] G. Mittal, V. Dhand, K. Y. Rhee, H. J. Kim, and D. H. Jung, "Carbon nanotubes synthesis using diffusion and premixed flame methods: A review," *Carbon Lett.*, vol. 16, no. 1, pp. 1–10, 2015, doi: 10.5714/CL.2015.16.1.001.
- [13] R. L. Vander Wal, L. J. Hall, and G. M. Berger, "Optimization of flame synthesis for carbon nanotubes using supported catalyst," *J. Phys. Chem. B*, vol. 106, no. 51, pp. 13122–13132, 2002, doi: 10.1021/jp020614l.
- [14] H. B. Abdullah, I. Ramli, I. Ismail, and N. A. Yusof, "Hydrocarbon sources for the carbon nanotubes production by chemical vapour deposition: A review," *Pertanika J. Sci. Technol.*, vol. 25, no. 2, pp. 379–396, 2017.
- [15] J. Z. Wen, M. Celink, H. Richter, M. Treska, J. B. Vander Sande, and M. Kraft, "Modelling study of single walled carbon nanotube formation in a premixed flame," *J. Mater. Chem.*, vol. 18, no. 13, pp. 1582–1591, 2008, doi: 10.1039/b717256g.